AIP | The Journal of Chemical Physics

Quantum mechanical calculations of state-to-state cross sections and rate constants for the F + DCl → Cl + DF reaction

Niyazi Bulut, Jacek Kłos, and Octavio Roncero

Citation: The Journal of Chemical Physics **142**, 214310 (2015); doi: 10.1063/1.4922110
View online: http://dx.doi.org/10.1063/1.4922110
View Table of Contents: http://scitation.aip.org/content/aip/journal/jcp/142/21?ver=pdfcov
Published by the AIP Publishing

Quantum mechanical calculations of state-to-state cross sections and rate constants for the F + DCl → Cl + DF reaction

Niyazi Bulut,[1,a)] Jacek Kłos,[2,b)] and Octavio Roncero[3,c)]
[1]*Department of Physics, Firat University, 23169 Elazig, Turkey*
[2]*Department of Chemistry and Biochemistry, University of Maryland, College Park, Maryland 20742-2021, USA*
[3]*Instituto de Física Fundamental (IFF-CSIC), C.S.I.C., Serrano 123, 28006 Madrid, Spain*

(Received 11 March 2015; accepted 24 May 2015; published online 5 June 2015)

We present accurate state-to-state quantum wave packet calculations of integral cross sections and rate constants for the title reaction. Calculations are carried out on the best available ground $1^2A'$ global adiabatic potential energy surface of Deskevich *et al.* [J. Chem. Phys. **124**, 224303 (2006)]. Converged state-to-state reaction cross sections have been calculated for collision energies up to 0.5 eV and different initial rotational and vibrational excitations, DCl($v = 0$, $j = 0 - 1$; $v = 1$, $j = 0$). Also, initial-state resolved rate constants of the title reaction have been calculated in a temperature range of 100-400 K. It is found that the initial rotational excitation of the DCl molecule does not enhance reactivity, in contract to the reaction with the isotopologue HCl in which initial rotational excitation produces an important enhancement. These differences between the isotopologue reactions are analyzed in detail and attributed to the presence of resonances for HCl($v = 0$, j), absent in the case of DCl($v = 0$, j). For vibrational excited DCl($v = 1$, j), however, the reaction cross section increases noticeably, what is also explained by another resonance. © *2015 AIP Publishing LLC.* [http://dx.doi.org/10.1063/1.4922110]

I. INTRODUCTION

Kinetic processes in nature can be sensitive to isotope substitution.[1,2] Very recently, Narevicius with coworkers observed the isotope effects in sub-kelvin reactions of metastable helium and hydrogen molecules.[3] Their application of the hydrogen isotopologue, deuterium, has allowed for the critical test of the potentials for that molecular system. Resonances are in general dependent on the isotopic substitution considered in a given reaction, specially at low energies affecting their widths by changing their position relative to their dissociation thresholds. These resonant features appear in other reactions, from H + HD, F + HD to F + HCl, but there is no unique resonance signature that shows up in all the reactions.[4]

The F + HCl/DCl reaction has been a subject of many theoretical[5–14] and experimental[15–17] studies. Experimental efforts, in general, have focused on the determination of thermal rate constants and product ro-vibrational state distributions for the F + HCl isotopologue. Zolot and Nesbitt[18] studied the state-to-state reaction dynamics under a single-collision condition (E_{col} = 4.3(1.3) kcal/mol) using crossed supersonic molecular beams technique. They found that the product rotational distributions display bimodal character that does not appear in previous flow and arrested-relaxation studies.[19,20] The bifurcational character of the rotational product distribution indicates complex dynamics in this molecular system due to possible quantum effects and non-adiabatic coupling between different electronic states.

The first *ab initio* potential energy surface (PES) for the F + HCl → Cl + HF reaction was calculated by Sayós *et al.*[5] using the spin-projected unrestricted second order Møller-Plesset level of theory (PUMP2) with the 6-311G(3d2f,3p2d) basis set. They constructed an analytical PES by fitting the *ab initio* points, introducing scaling factors around the transition state points to reproduce experimental rate constants. Their effective barrier height, of 1.12 kcal/mol, for the F + HCl reaction is similar to that of the empirical LEPS[20] surface. Quasi-classical trajectory (QCT)[6] and wave packet (WP) simulations have been carried out[7] on this PES.

Deskevich *et al.*[8] reported a new global three-dimensional high level *ab initio* PES for the lowest $1^2A'$ adiabatic state (hereafter called DHSN PES). This PES has been obtained from dynamically weighted state-averaged multi-reference self-consistent field calculations (dw-SA-MCSCF) followed by the internally contracted multi-reference configuration interaction method with Davidson correction (ic-MRCISD+Q) with complete basis set extrapolation. In addition, the correlation energy has been scaled, to reproduce the experimental exothermicity of −1.4336 eV.

Both surfaces, the one of Sayós *et al.*[5] and the DHSN PES,[8] have a bent transition state geometry, with F–Cl–H angles of 131.2°and 123.5°, respectively. The transition state's barrier height on the DHSN PES is 0.1647 eV. This can be compared to Sayós' unscaled PUMP2 PES barrier height of 0.205 eV and PUMP4 one of 0.1738 eV.[5] All these values are higher than the experimentally estimated barrier height of 1.08 kcal/mol (0.046 83 eV) (see discussion in Li *et al.*[13]).

The first theoretical reaction probabilities on the DHSN PES were calculated by Hayes *et al.*[9] employing the QCT

a)nbulut@firat.edu.tr
b)jklos@umd.edu
c)octavio.roncero@csic.es

and time-independent close-coupled hyperspherical quantum methods. The calculated reaction probabilities were found to be strongly dependent on the initial rotational state of the HCl. The probabilities showed an enhancement of reactivity upon rotational excitation of the HCl molecule. Employing the DHSN PES, Sun *et al.*[21] performed a new time-dependent quantum wave packet simulations to study the influence of reagent ro-vibrational excitation on the dynamics of the F + HCl/DCl reactions.

In 2009, Defazio and Petrongolo[12] performed time-dependent real wave packet (RWP) calculations for the F + HCl reactive collisions on the DHSN PES. They calculated initial-state reactive cross section for many rotational excitations, j_0, and found that it increases with j_0. They also found the importance of steric effects in F + HCl reaction, where the reactivity is enhanced by low K values, with K being the projection quantum number of the total angular momentum (J). These calculations were performed using the centrifugal sudden (CS) approach for HCl($j_0 = 0, \ldots, 16$). For the case of initial $j = 0$, they performed coupled-channels (CC), finding important changes with CS results. They concluded that converged CC calculations need to be done for this reaction.

This was done more recently by Bulut *et al.*[22] where also state-to-state integral cross sections (ICS) were calculated using a wave packet method. In that work, final-state product resolved reaction probabilities were calculated to investigate the origin of a broad local maximum in the shoulder of $v = 0$, $j = 0$, and $J = 0$ reaction probabilities. First accurate integral cross sections and rate constants have been calculated and compared with the available experimental data. It was found that the accurate rate constant calculated by using wave packet method was lower than the experimental value and it was concluded that the reaction barrier on the DHSN PES was too large.

In the most recent work, time-dependent wave packet (TDWP) and time-independent quantum methods (TIQM) were used to investigate state-to-state collision dynamics for the F + HCl reaction by Li *et al.*[13] In that work, vibrational and rotational state distributions were calculated at selected collision energies and compared with the experimental data of Nesbitt's group.[18] The experimental data were measured at a constant temperature of 50 K. The obtained theoretical distributions agreed almost quantitatively with the experimental vibrational populations,[13] with the populations of $v = 3$ vibrational state of the HF product being overestimated by theory.

Here, in this work, we revisit the model heavy-light-heavy (HLH) hydrogen exchange type reaction, F + DCl → Cl + DF, where the hydrogen atom is replaced with deuterium isotope. The work focuses on the understanding the differences with the F + HCl → Cl + HF isotopologue reaction, in which results were obtained previously by some of us,[13,22] to investigate the isotopic effect. We show calculations for the first two initial vibrational states of the DCl molecule, $v = 0$ and 1, and for the two lowest initial rotational states. As has been done previously for the F + HCl reaction,[22] we have employed the DHSN PES in the reactive scattering calculations presented in this work. Time dependent wave packet calculations and time independent close-coupling ones are performed neglecting the open-shell structure of F and Cl atoms and on a single lowest Born-Oppenheimer adiabatic PES. Therefore, there are no non-adiabatic nor spin-orbit coupling effects studied in this work.

The paper is organized as follows. Section II describes the methods used in the scattering calculations to obtain reactive cross sections and rate constants. Results and their discussion are presented in Sec. III, and finally with Sec. IV concluding this work.

II. COMPUTATIONAL METHODS

The F + HCl/DCl($v = 0, 1, j = 0, 1$) → Cl + HF/DF reaction is a prototype HLH reaction and has been studied using wave packet methodology since the last decade.[7,12,21] In this H + LH′ → HL + H′ reactions, one of the principal axes of inertia is nearly parallel to the H–H′ internuclear vector, and only few helicities need to be included when using either reactant or product Jacobi coordinates. However, the skew angle is pretty small, and the description of final states of products using reactant coordinates would require very dense grids, making very expensive the calculation. For these two reasons, it has been demonstrated that for H + LH′ → HL + H′ reactions it is more efficient to use product Jacobi coordinates.[23]

In this work, the state-to-state reaction probabilities were calculated using a wave packet method, with the MADWAVE3 code described by Zanchet *et al.*[24] The MADWAVE3 code has been implemented to many atom-diatom collisions,[25] well documented in the literature[24,26] and only the details relevant to the present work will be given here. In the present calculations, the initial wave packet is located in the asymptotic reactant channel where there is no influence of the interaction potential. This initial wave packet is transformed to products Jacobi coordinates, in which the grid of the calculation is defined to perform the propagation and the determination of the state-to-state probabilities. The grid used was optimized to produce converged results, minimizing the effects of the absorption parameters at the edges of the radial grids. For this purpose, the normalized total flux in all the exit channels was calculated to be ≈1, with an error lower than 1% for the energy range of interest. The parameters used for the wave packet calculations are listed in Table I and were the same for all initial states of the reagents.

The exact calculations of reaction probabilities at $J > 0$ would demand including all possible values of Ω' projections for a given total angular momentum J. The helicity basis

TABLE I. Parameters used in the wave packet calculations (all distances are given in Å units).

Reactant scattering coordinate range:	$R_{min} = 0.001$; $R_{max} = 14.5$
Number of grid points in R:	512
Diatomic coordinate range:	$r_{min} = 0.1$; $r_{max} = 14.5$
Number of grid points in r:	240
Number of angular basis functions:	264
Center of initial wave packet:	$R_0 = 10.0$
Initial translational kinetic energy/eV:	$E_c = 0.558$
Analysis point:	$R = 9.0$
Number of Chebyshev iterations:	40 000

used in this work has been truncated in such a way that $0 \leq |\Omega'| \leq \min(J, |\Omega'_{max}|)$, with $\Omega'_{max} = 20$ in the present calculations.

The calculation of state-to-state ICS as a function of collision energy for an initial ro-vibrational DCl state v, j, to yield DF($v'j'$) products $\sigma_{v,j\to v'j'}(E_c)$, requires summation of all the partial wave contributions of the total angular momentum J to the reaction probabilities as[27,28]

$$\sigma_{v,j\to v'j'}(E_c) = \frac{\pi}{k^2}\frac{1}{2j+1}\sum_{J=0}^{J_{max}}\sum_{\Omega\Omega'}(2J+1)P^J_{vj\Omega\to v'j'\Omega'}(E_c), \tag{1}$$

where $k^2 = 2\mu_r E_c/\hbar^2$, and $P^J_{v,j,\Omega\to v'j'\Omega'}(E_c) = \left|S^J_{v',j',\Omega'\ v,j,\Omega}\right|^2$ is the reaction probability from the initial ro-vibrational state (v, j, Ω) to given final state (v', j', Ω') of products and depends on the collision energy, E_c, at the total angular momentum J. The total reaction integral cross section is readily obtained by summing over all final (v', j') states of products as

$$\sigma_{v,j}(E_c) = \sum_{v'j'}\sigma_{v,j\to v'j'}(E_c). \tag{2}$$

In order to get convergence for $E_c = 0.5$ eV, the summation in Eq. (1) needs to be performed up to $J_{max} = 110$. In order to reduce the computational effort, only $J = 0, 5, 10, \ldots, 110$ (in steps of 5) were calculated. The rest of the reaction probabilities for intermediate total angular momenta were obtained by an interpolation procedure based on the J-shifting approach.[29] Therefore for a given $J \in [J_1, J_2]$, the reaction probabilities were obtained as[25,30]

$$P^J(E_c) = \frac{J_2 - J}{J_2 - J_1}P^{J_1}(E_c - B[J(J+1) - J_1(J_1+1)]) + \frac{J - J_1}{J_2 - J_1}P^{J_2}(E_c + B[J_2(J_2+1) - J(J+1)]), \tag{3}$$

where E_c is the collision energy and the rotational constant B is previously fitted. The rotational constant used in this expressions was fitted for each (J_1, J_2) interval considered, by setting $P_{J_2} = P^{J_1}(E_c - B[J_2(J_2+1) - J_1(J_1+1)])$ for the total reaction probabilities. The convergence of the cross section using this J-shifting interpolation method was checked to be better than 1% by considering two J_2–J_1 intervals, 5 and 10.

Initial-state resolved rate constants, $k_{v,j}(T)$, in the temperature interval between 100 K and 400 K were calculated from the state-specific excitation functions, $\sigma_{v,j}$, using the standard formula,

$$k_{v,j}(T) = \left(\frac{8}{\pi\mu_r(k_BT)^3}\right)^{1/2}\int_0^\infty E_c\,\sigma_{v,j}(E_c)e^{-E_c/k_BT}\,dE_c \tag{4}$$

with $v = 0, 1$ and $j = 0, 1$. Only $j = 0$ is taken into consideration for $v = 1$.

III. RESULTS AND DISCUSSION

In order to check the convergence of the TDWP results, Close-Coupling TIQM (TIQM-CC) calculations for partial waves $J = 0, 40$, and 90 have been performed with the quantum ABC reactive scattering program,[31] using the parameters listed in Table II. The wave packet and TIQM reaction probabilities for the DCl(v = 0, j = 0) + F collision are shown in Fig. 1. The excellent agreement between the two sets of results is taken as a proof of the convergence of the TDWP in the whole energy interval, similar to that reported previously.[13,22] For $J = 0$, the reaction shows a threshold at ≈0.2 eV due to the barrier in the entrance channel of the PES. After the threshold, the reaction probability increases monotonously with energy, behavior characteristic of a direct reaction with a barrier. As the total angular momentum J increases, total reaction probabilities shift to higher collision energy because the centrifugal barrier increases as well, as expected.

TABLE II. Parameters used in the time-independent F + DCl ABC[31] calculations for two partial waves $J = 0$ and $J = 90$.

	$J = 0$	$J = 90$
Hyperspherical maximal radius R_{max}/Å `rmax`:	23.8	23.8
Number of grid points in r:	560	560
Number of basis functions:	379	3283
Maximum projection quantum number `kmax`:	0	10
Maximum rotational quantum number `jmax`:	25	25
Energy for basis cut/eV `emax`:	1.6	1.6

The reaction threshold for HCl($v = 0, j = 0$) + F and $J = 0$[22] is shifted to lower energies as compared to the deuterated species, as shown in Fig. 1. This may be explained by the isotopic effect on the zero-point energy (ZPE), which is reduced when increasing the reduced mass. This affects not only the diatomic reagents but also the transition state (TS). In this last case, the ZPE is not strictly defined, since it corresponds to the degrees of freedom perpendicular to the reaction coordinate, and they are not completely separated and there is always a coupling between them. If we neglect it, the shift in the reaction

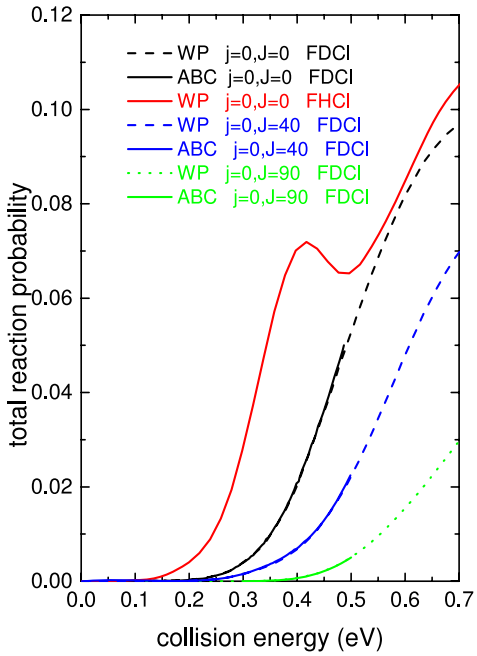

FIG. 1. Total reaction probabilities as a function of collision energy calculated using the time-dependent WP method and time-independent quantum close-coupling (ABC) results for selected total angular momentum J values at initial ro-vibrational state of the DCl($v = 0, j = 0$) reagent for the title reaction.

threshold, Δ, is related to the change between the ZPE of the reagents and TS, by $\Delta = ZPE_{TS} - ZPE_{reag}$.

In addition to the ZPE effect, this shift may be due to the channel in the tunneling probability, which decreases with increasing mass. This tunneling can also create resonances at which reactivity increases with reducing the reduced mass. These may explain the resonance appearing for HCl and not for DCl. The presence of van der Waals minima in the entrance and exit channels of the F + HCl/DCl reactions will give rise to Feshbach resonances that were studied in detail previously by Quéméner and Balakrishnan.[10] These cold/ultracold regime features are out of scope of this work. This resonance appearing in HCl at ≈0.4 eV, very close to the reaction threshold, has been reported previously[13,22] and has a large half-width, of ≈0.1 eV, associated to a short lifetime of ≈3 fs, which is shorter than the typical vibrational period. This peak is very similar to that appearing for the F + HD reaction in the HF channel,[4] but it presents two important differences: the peak is considerably broader (0.1 eV in F + HCl versus 0.013 eV in F + HD) and it is immersed in the background envelope associated to the direct reaction above reaction threshold. These two features make more difficult a clear assignment of the resonance through the use of pseudo-spectral methods[32] and stabilization methods[33] as already reported for the F + HD reaction.[4,34]

The wave function at a given energy can be obtained from wave packet propagations using common pseudo-spectral methods as[4,32,35]

$$\Psi_E = \frac{1}{2\pi\hbar a(E)} \int dt e^{iEt/\hbar} \Psi_t \tag{5}$$

or equivalently using a modified Chebyshev propagator[36]

$$\Psi_E = \frac{1}{2\pi\hbar a(E)} \sum_k c_k(H_s, E) \Psi_k, \tag{6}$$

as it is done here, where Ψ_k is the k-estimate Chebyshev component of the wave packet and the coefficient is C_k which depends on the energy and the scaled Hamiltonian.[36]

The density probability of some of the these wave functions is shown in Fig. 2 for $E_c = 0.4$, 0.5, 0.6, and 0.7 eV, respectively. This kind of H + LH′ → HL + H′ reactions has a very small skew angle, and as a consequence, the reaction occurs at Jacobi angles close to collinear configuration, and only few angles in a small range around $\gamma = \pi$ are shown. In this figure, it can be seen that for $E_c = 0.4$ eV, corresponding to the top of the peak of the reaction probability at $J = 0$, the wave function in the reactant and product channels is connected through the saddle point region, and it corresponds to $v = 0$ in the F + HCl reactant channel and to $v' = 3$ in the Cl + HF product channel. For $E_c = 0.5$ and 0.6 eV, it seems that the probability density between the reactant and product channels becomes closer to zero, what demonstrates why the associated reaction probability decreases. Also, the density in the product channels for these two energies is not so clearly assigned to $v' = 3$, but it corresponds to a mixture. For $E_c = 0.7$ eV, the connection between reactant and product channels seems to be restored explaining again the raise of the reaction probability.

Following the method of Fano, for an isolated resonance case, the exact wave function can be expressed as an expansion in terms of the bound, Φ_i, and continuum, $\Phi_{\beta E}$, solutions of a zero order Hamiltonian as

$$\Psi_{\alpha E} = a_i(E)\Phi_i + \sum_\beta \int dE' b_{\alpha E}^{\beta E'} \Phi_{\beta'}, \tag{7}$$

where $a_i(E)$ is usually given by a Lorentzian-like profile.[37] For narrow resonances, the bound component Φ_i becomes dominant at the energy of the resonance, and it is therefore possible to assign a bound state to the resonance.[33] In this case, however, the resonance is very broad, as commented above, and the bound and continuum components of the wave function are of the same magnitude, what makes very difficult a clear identification of the bound part. Several attempts have been done using propagations in different set of coordinates, leading to similar qualitative results.

This resonance is present for higher total angular momentum J in the F + HCl ($v = 0, j = 0$) case, as shown in the bottom panel of Fig. 3. There is a peak at ≈0.41 eV from $J = 0$ to 20, which corresponds to the resonance discussed above for $J = 0$. This peak is absent for F + DCl ($v = 0, j = 0$), in the top panel of Fig. 3, for which the reaction probability shows a monotonous decrease as a function of J. This is the reason why the reaction ICS for DCl($v = 0, j = 0$) is approximately two times lower than for HCl($v = 0, j = 0$), shown in the bottom panel of Fig. 4.

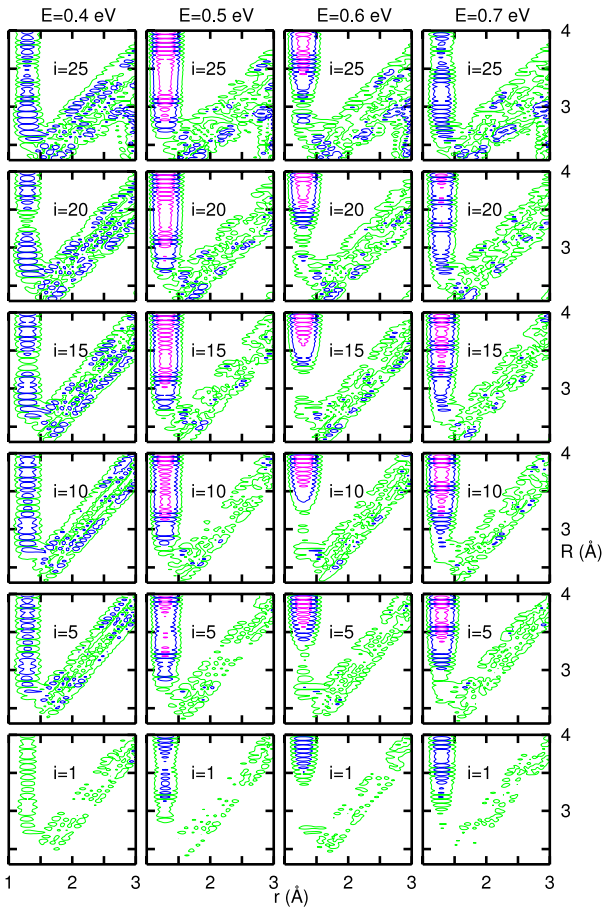

FIG. 2. Wave functions at fixed energies (indicated in the top of the panels) obtained for F+HCl collisions using Eq. (6) in a wave packet calculation in reactant Jacobi coordinates. The label i denotes the point of the Gauss-Legendre quadrature grid of 300 points used, i.e., $\gamma = 179.5414$, 177.153 15, 174.1589, 171.1642, 168.1693, and 165.1744 for i = 1, 5, 10, 15, 20, and 25.

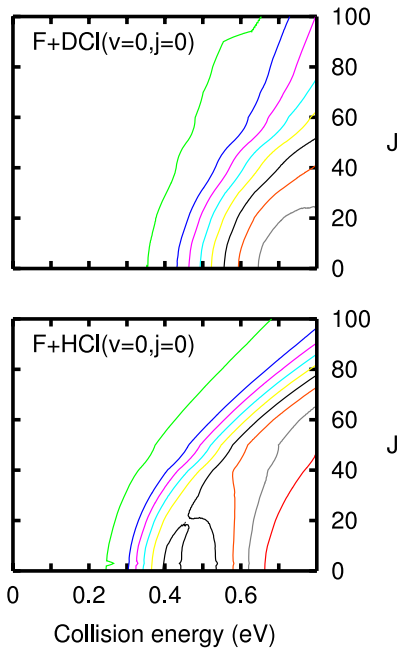

FIG. 3. Contour plot of the reaction probability for HCl(v = 0, j = 0) + F and DCl(v = 0, j = 0) + F collisions, as a function of collision energy and total angular momentum, J. The contours start in 0.01 in intervals of 0.01.

There is another important difference in the effect of the initial rotational excitation of the HCl and DCl molecules. One rotational quantum in HCl increases the ICS roughly by a factor of two, while for DCl, there is no effect, as shown in Fig. 4. This difference can again be attributed to the presence of the same resonance, as well as to higher energy resonances which appear for higher j values. In Fig. 3 of Ref. 22, all the reaction probabilities obtained for HCl($v = 0, j = 0, 1, 2, \ldots, 16$) and $J = 0$ show peaks associated to resonances similar to those reported here for HCl($v = 0, j = 0$) in Fig. 1 which support this argument.

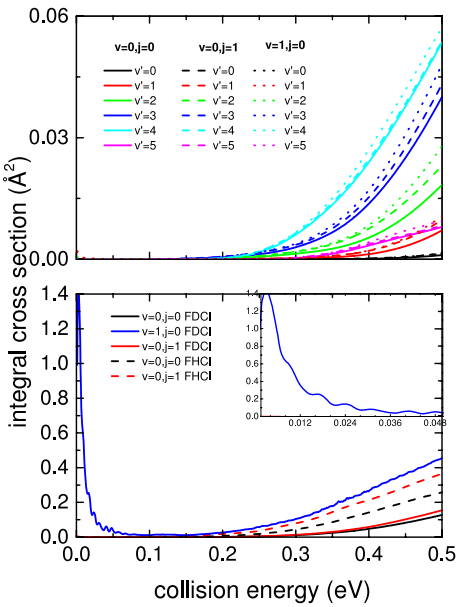

FIG. 4. Vibrationally resolved integral cross sections for the F + DCl($v = 0, j = 0-1$) → Cl + DF(v') and F + DCl($v = 1, j = 0$) → Cl + DF(v') reactions (top panel). The bottom panel shows the total integral cross sections for given initial ro-vibrational state of F + H/DCl reaction.

TABLE III. Selected reactant and product ro-vibrational channel energies for F + HCl and F + DCl reactions. Energy unit expressed in eV. Italicized values for each isotopologue reaction indicate the closest channels in energy enabling small gap pathways that increase the reactivity.

F + HCl (v, j)			FH(v', j') + Cl		
v	j	Energy	v'	j'	Energy
0	0	*0.185 15*	0	0	−1.229 42
0	1	*0.187 73*	0	1	−1.224 30
0	2	*0.192 91*	1	0	−0.734 77
0	3	0.200 66	2	0	−0.261 19
0	4	0.211 00	3	0	*0.192 58*
1	0	0.544 26	4	0	0.627 49
F + DCl (v, j)			FD(v', j') + Cl		
v	j	Energy	v'	j'	Energy
0	0	*0.133 15*	0	0	−1.299 38
0	1	0.134 48	0	1	−1.296 68
0	2	0.137 15	0	2	−1.291 27
0	3	0.141 16	1	0	−0.936 44
0	4	0.146 51	2	0	−0.584 87
1	0	*0.393 63*	3	0	−0.244 13
2	0	0.646 72	4	0	*0.086 23*
3	0	0.892 88	5	0	*0.406 60*

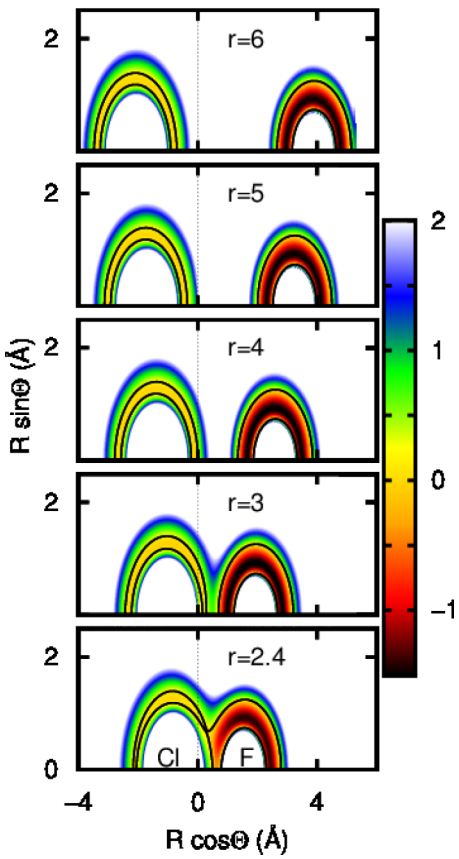

FIG. 5. Contour plot of the FCl–H potential for different r_{FCl} distances. Energy in eV, and the solid line corresponds to 0.17 eV to indicate the position of the saddle point. F and Cl atoms are being placed in the X axis, with the center of mass at the origin, while the position of the H atom is indicated by X = RcosΘ and Y = RsinΘ, R being the distance of H to the FCl center of mass, and Θ is the angle between R and the FCl internuclear vector.

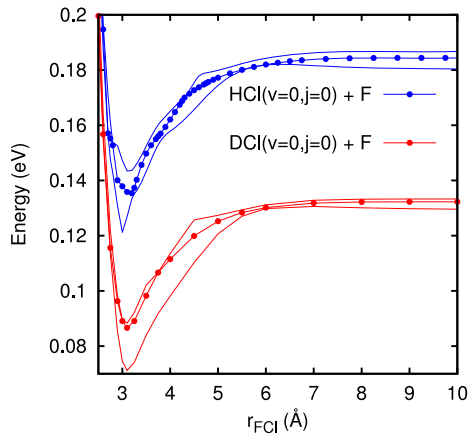

FIG. 6. Two-dimensional adiabatic eigenvalues obtained for several r_{FCl} distances, for the case of HCl+F and DCl+F. For simplicity, only three consecutive roots are shown for each case. The two higher roots correlate to the HCl($v=0, j=0$ and 1) and DCl($v=0, j=0$ and 1) states for $r_{FCl}=10$ Å. These roots are the 61 and 116 for HCl and DCl, respectively. For HCl+F, the 60th root corresponds to HF($v=3, j=1$). For DCl+F, the 115th root corresponds to HF($v=4, j=7$) (see eigenfunction amplitudes in Fig. 7).

These resonances do not appear for the two rotational states of DCl($v=0$, $j=0$ and 1) which explains why the ICS is lower and why there is no change when increasing the rotational excitation of DCl. However, for DCl($v=1$, $j=0$), the ICS shows a peak at the threshold, and for higher energies, it is of the order of that obtained for HCl($v=0$, $j=1$). This again shows that the appearance of broad resonances at energies close to the threshold yields considerably larger ICS.

But when do these resonances appear and what is their origin? One clue is provided in Table III. In all cases, these resonances seem to appear when the initial vibro-rotational energy of the reactants, E_v, nearly coincides with that of products, $E_{v'}$. This happens for HCl($v=0$)/HF($v'=4$)-HCl($v=0$)/HF($v'=3$) and DCl($v=1$)/DF($v'=5$).

In order to build a simple model, we shall consider the H + LH → HL + H character of these two reactions, with very small skewing angles, $\beta = 16°$ and 22°, for HCl and DCl, respectively. Since F and Cl have masses considerably larger than H or D, their velocity may be considered to not change along the collision. Thus, when the reaction takes place, all the available energy of this exothermic reaction goes into the H atom, in the form of vibrational and/or rotational excitation. That is, the slow relative translational motion between the two heavy atoms, F and Cl, can be approximately separated adiabatically from the fast motion of the H atom,[38–40] in analogy to the Born-Oppenheimer approximation.

For doing this adiabatic separation, another set of Jacobi coordinates is chosen, with $\mathbf{r}_{FCl}$ being the F–Cl internuclear vector and $\mathbf{R}_H$ being the vector from the FCl center of mass and the H atom, and γ_H the angle between them. The contours of the PES for several r_{FCl} distances are shown in Fig. 5, showing the typical attractive rings around the heavy atoms, for long r_{FCl} distance. As the two heavy atoms get closer, the two rings superimpose, allowing the transfer of the hydrogen atoms from one to another, and the saddle point is found for $r_{FCl} \approx 2.4$ Å.

For $J=0$, the two-dimensional eigenvalues are obtained for different r_{FCl} values. A grid formed by 1200 point in R_H and 600 angles γ_H is used to represent the two-dimensional system,

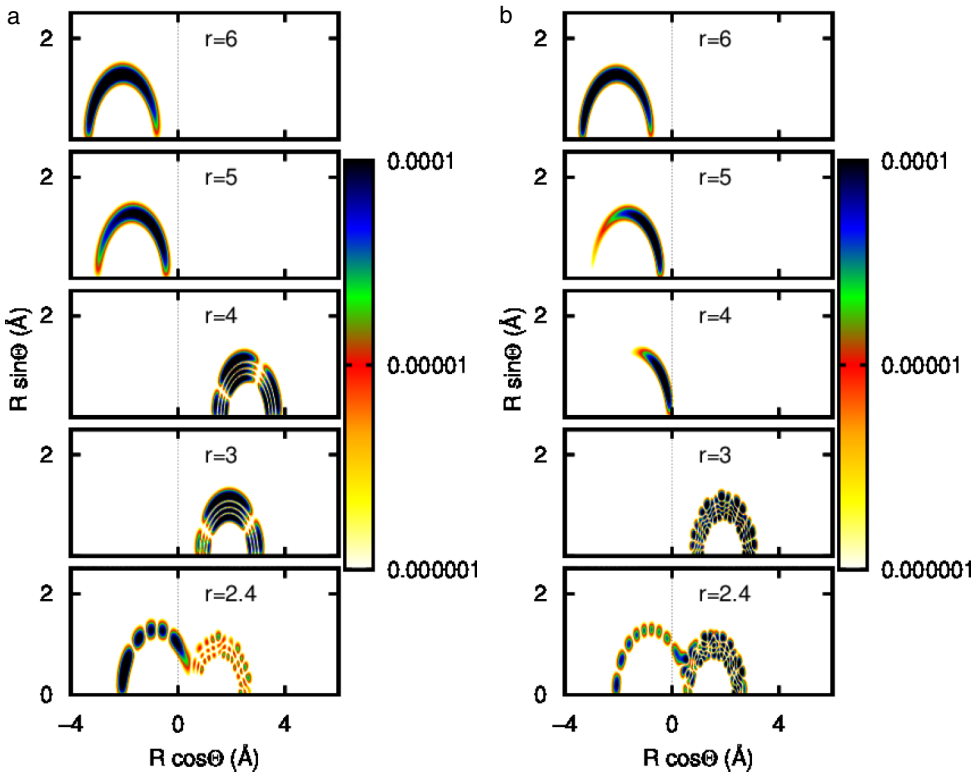

FIG. 7. Contour plot of the amplitude of two-dimensional eigenvectors obtained for the F+HCl (a) and F+DCl (b) reactions at different r_{FCl}, correlating to HCl($v=0, j=0$) and DCl($v=0, j=0$), respectively.

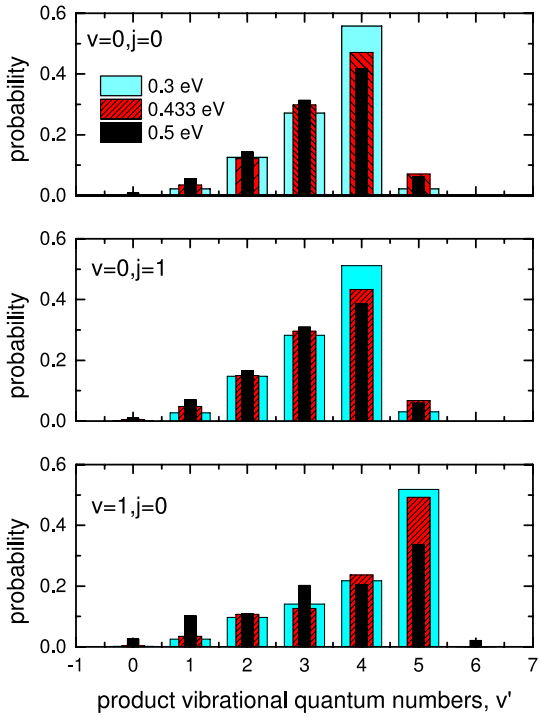

FIG. 8. Product vibrational state-resolved cross sections for the F+DCl(v, $j=0$) → Cl+DF reactions.

and the kinetic terms of the Hamiltonian are evaluated using a sinc and Gauss-Legendre discrete variable representation (DVR) method. The eigenvalues are obtained using an iterative non-orthogonal Lanczos method. Details about the bound state calculations can be found in Ref. 41.

The resulting eigenvalues as a function of the $\mathbf{r}_{FCl}$ distance give rise to the spaghetti-type curves typically associated to hyperspherical coordinates, shown in Fig. 6 for three eigenvalues of F + HCl and F + DCl. The eigenvalues with circles correspond to HCl($v=0, j=0$) and DCl($v=0, j=0$) at long distance, being the 61 and 116 roots, respectively. The other two are the closest eigenvalues, included to make the crossings more evident. The vibrational frequency of DF is smaller than that of HF, and therefore the density of states is expected to be higher for DCl than for HCl. However, the curve correlating to DCl($v=0, j=0$) is smoother and shows less avoided crossings than that of HCl($v=0, j=0$). The reason is the smaller energy difference between HCl($v=0, j=0$) and HF($v'=3, j=0$) than for DCl($v=0, j=0$) and DF($v'=4, j=0$), in Table III. The reduced mass of HCl and HF (or DCl and DF) is very similar and $\approx m_H$ (or m_D). This explains why the rotational constants of reactants and products are relatively similar as well. Thus, near the degeneracy between HCl($v=0, j=0$) and HF($v'=3, j=0$), there are several rotational states in the two rearrangement channels which become very close in energy, giving rise to several curve crossings. On the contrary, DCl($v=0, j=0$) eigenvalue is close to a higher rotational DF($v=4, j>>$), with a larger rotational spacing, and therefore DCl($v=0, j=0$) is facing a lower density of DF states giving rise to a smoother adiabatic potential energy.

Within the model for this HL + H → H + LH reaction, fast motion of H/D atom is adiabatically adapting to the potential at each distance r_{FCl}. The amplitude densities of the two-dimensional eigen-states at frozen r_{FCl} distance are shown in Fig. 7 for r_{FCl} in Fig. 1 equal to 6 and 5 Å, in which the amplitude density moves towards the region between F and Cl. The effect is more pronounced in DCl because it experiences smaller changes in the interaction potential due to its smaller ZPE. The crossing at $r_{FCl} \approx 6$ Å in Fig. 6 in both cases does not seem to be effective since it does not change the eigenvectors.

On the other hand, at $r_{FCl} \approx 4$ Å, there is a crossing between HCl($v=0, j=0$) and HF($v'=3, j'=2$), while in the deuterated case, this crossing occurs at shorter distance, $r_{FCl} \approx 3$ Å, with DF($v'=4, j'=15$). At these two distances, there is a relatively high barrier for H/D exchange between Cl and F atoms, and at these crossings, the two degenerate states may present a tunneling probability and form tunneling resonances, similar to findings for FHD reported earlier by Skodje[4] The deuterium has larger mass and for DCl($v=0$, $j=0$) less degeneracies, forming lower number of resonances in comparison to HCl.

Finally, at shorter r_{FCl} distances, the barrier disappears and the wave function of H/D spreads around the two heavy atoms, as shown for the saddle point at $r_{FCl} = 2.4$ Å. These wave functions change rapidly as the system gets closer to the repulsive part of the spaghetti, where more non-adiabatic transitions between different channels will rise due adiabatic curves getting closer. The nature of the wave functions at these distances shows a marked preference for the final vibrational state $v'=2$ for HF, and $v'=4$ for DF, respectively.

This adiabatic picture explains the inverse vibrational populations of DF products, in Fig. 8, and that previously reported for HF in Refs. 13 and 22. In a work of Quéméner and Balakrishnan[10] on cold and ultracold F + HCl and F + DCl reactions, similar effects were observed of the enhanced reactivity for the final $v'=4$ vibrational product state from the initial $v=0$ state. In the case of F + DCl ($v=1, j=0$), there is a near-degeneracy with DF($v'=5, j'=0$), which explains why the ICS in Fig. 4 increases approximately by a factor of 5 with respect to that of F + DCl ($v=0, j=0$). Also, it explains why the final vibrational distribution of DF products is so markedly peaked at the higher $v'=5$ channel.

Product's final rotational state-resolved integral cross sections at three selected collision energies (0.3, 0.43, and 0.5 eV) are shown in Figure 9 for the title reaction. For the $v=0, j=0-1$ initial states in all panels, the larger cross section corresponds to the $v'=4$ DF product vibrational state and for the same $j' \approx 16$, independently of the collision energy and the initial rotational state. The initial vibrational excitation of the HCl reactant to the $v=1, j=0$ state places the energy of the reactants above the height of the reaction barrier; therefore, the reaction does not have to proceed through the bent transition state that can cause the hot rotational distribution. For the initial $v=1, j=0$ state, the rotational distribution of the DF product becomes substantially colder and the peak of the distribution is shifted towards lower j' values. The final vibrational distribution was explained above within the adiabatic model. The fact that the peak in the final rotational quantum number is always at the same j' value may be related to the presence of the resonance. For lower v' values, the rotational distributions are less structured but they are all rather similar changing collision energy and initial rotational state. The more notorious change

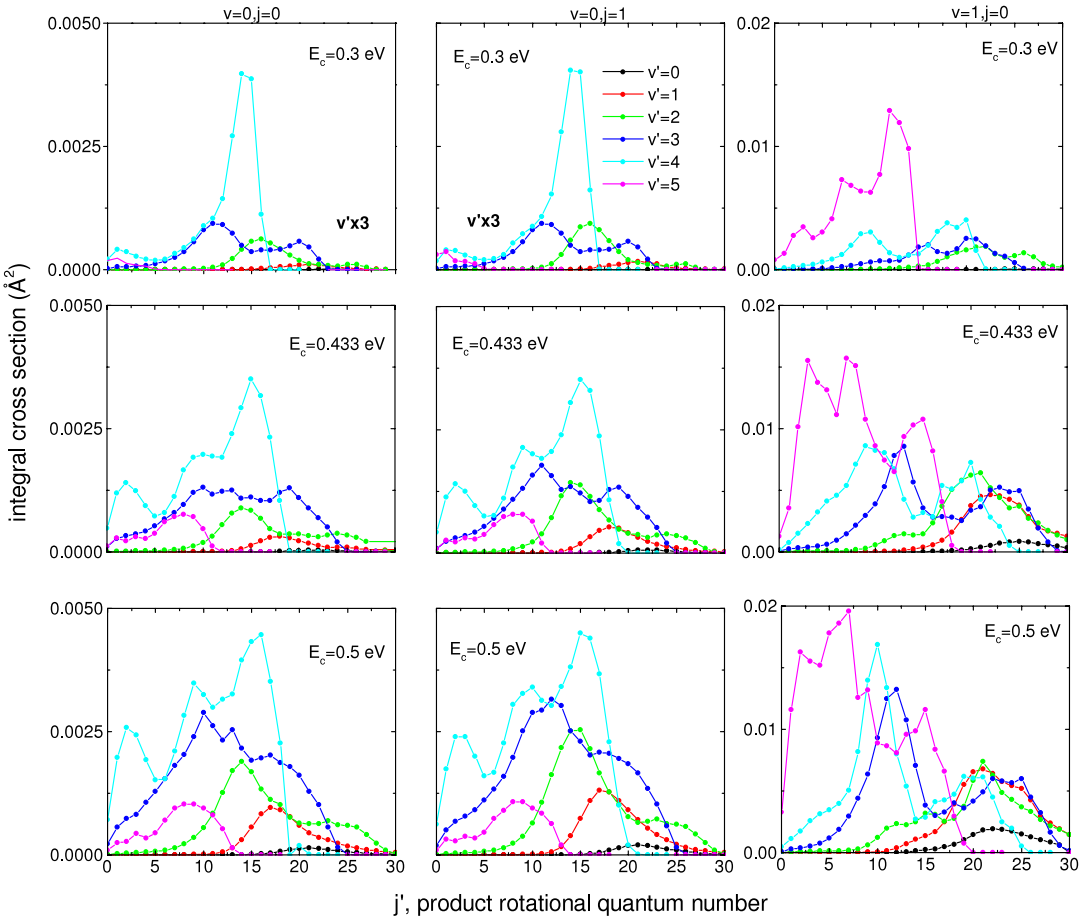

FIG. 9. Product rotational state-resolved integral cross sections for the F + DCl($v = 0, j = 0 - 1$) → Cl + DF and F + DCl($v = 1, j = 0$) → Cl + DF reaction.

is the appearance of several maxima for $v' = 4$ at $j' = 3$, 9, and 15, at higher collision energies (0.43 and 0.5 eV). These multimodal character of the rotational distribution could be tentatively associated to the increase of the number of curve crossings among the initial and product channels as collisional energy increases. At each crossing, a dominant rotational state of the products is formed. During the evolution of these wave packets to form products, several transitions are expected to occur leading to interference patterns which could explain the appearance of several maxima and minima in the rotational distribution. In any case, this complex distribution can be taken as a clear evidence of a complex reaction dynamics.

Initial ro-vibrational state specific rate constants are presented in Figure 10. In the top panel of the figure, final product's vibrational state-resolved rate constants for the F + DCl reaction are displayed for the three initial ($v = 0$, $j = 0$), ($v = 0$, $j = 1$), and ($v = 1$, $j = 0$) rotational states. The reaction rate constants for the $v' = 5$ and the $v' = 6$ final vibrational states out of the initial $v = 0, j = 0 - 1$ and $v = 1, j = 0$ states are already very small, respectively. As can be seen in the figure, the initial $j = 1$ rotational state does not have a big effect on the rate constant but the initial $v = 1$ vibrational state has, as expected from the integral cross sections depicted in the bottom panel of Figure 4. In the bottom panel of Figure 10, the initial state-resolved total rate constants slightly changing with the temperature, monotonically increasing with the temperature, which is a characteristic behavior of a reaction with a

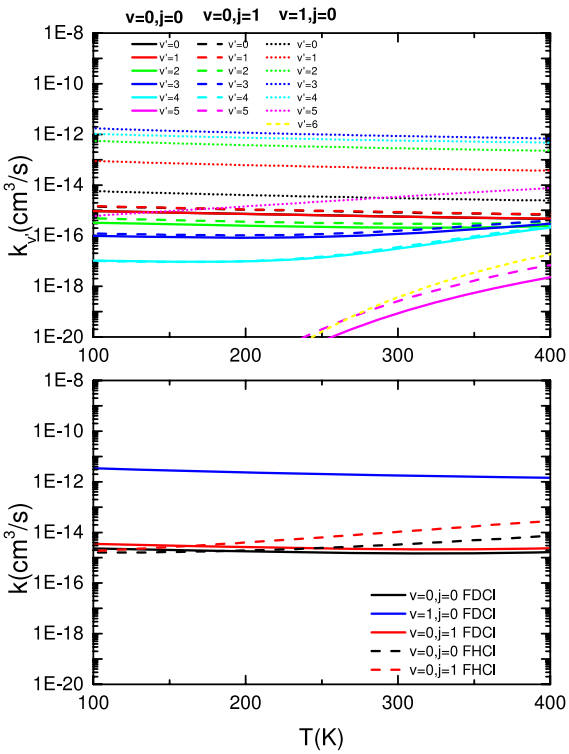

FIG. 10. Product vibrational-state resolved (top panel) F + DCl and initial state-selected (bottom panel) F + H/DCl rate constants.

barrier. The F + DCl initial state rate constants in this panel are approximately two to three orders of magnitude smaller in the higher temperature region than corresponding rates for the F + HCl reaction.[22] For the temperatures between 100 and 200 K, they become similar for the initial state $j = 0$ and $j = 1$. For the $v = 1$, $j = 0$ initial ro-vibrational state, the F + DCl reaction is much more exothermic and the rate constant for this initial state is practically constant in the temperature range considered in this work.

IV. CONCLUSIONS

We have carried out quantum scattering calculations for the $F + DCl(v, j) \rightarrow Cl + DF(v', j')$ reaction in the collision energy range from a threshold up to 0.5 eV. We have compared reaction probabilities for selected partial waves obtained from the time-dependent wave packet and the time-independent quantum scattering methods and we found an excellent agreement. We have investigated the effect of different initial ro-vibrational states of the DCl on the F + DCl reactivity. Our new F + DCl results are compared with those previously calculated by some of us for the F + HCl reaction. For DCl($v = 0, j = 0,1$), the cross sections calculated here are about two times smaller than those reported previously for HCl reaction. Also, it is found here that there is no effect of the rotational excitation of the DCl reagent on the cross section, while for HCl, a considerable reactive enhancement was found when exciting the rotation of HCl molecule.

These differences are attributed to the resonance near threshold, at $E_c = 0.4$ eV, appearing in the F + HCl ($v = 0, j$) reaction, and absent in the case of F + DCl ($v = 0, j$). A detailed investigation is done to explain the origin and the role of this resonance. On the other hand, we found that the initial vibrational excitation of the DCl reactant increases the reactivity to a great degree.

We present also final vibrational distributions of the DF products in the F + DCl reactions from $v = 0$ and $v = 1$ states and explain the propensity towards final $v' = 4$ or $v' = 5$ vibrational channels, respectively. The rotational distributions of the DF products are also presented for three selected collision energies. They have usually single ($v' = 2$) or bimodal or trimodal for other final vibrational states. Finally, we have presented initial state rate constants obtained from the excitation functions for the F + DCl reaction.

ACKNOWLEDGMENTS

We would like to thank Millard H. Alexander for his encouragement for this project and fruitful discussions. Financial support from the Scientific and Technological Research Council of TURKEY (TUBITAK) (Project No. TBAG-112T827) is gratefully acknowledged. Computations have been done on the High Performance and Grid Computing Center (TR-Grid) machine at ULAKBIM/TURKEY. O.R. has been supported by the Ministerio de Economía e Innovación under Grant Nos. CSD2009-00038 and FIS2011-29596-C02 and used the CESGA computing centre under computing ICTS grants and also acknowledge the Chemistry and Molecular Sciences and Technologies COST Action CM1401. J.K. is grateful for the financial support from the U.S. National Science Foundation (Grant No. CHE-1213332 to M. H. Alexander). O.R. and N.B. also acknowledge CSIC for a travelling Grant No. I-LINK0775.

[1]E. W. Washburn and H. C. Urey, Proc. Natl Acad. Sci. U. S. A. **18**, 496 (1932).
[2]F. H. Westheimer, Chem. Rev. **61**, 265 (1961).
[3]E. Lavert-Ofir, Y. Shagam, A. B. Henson, S. Gersten, J. Kłos, P. Żuchowski, J. Narevicius, and E. Narevicius, Nat. Chem. **6**, 332 (2014).
[4]R. T. Skodje, Adv. Quantum Chem. **63**, 119 (2012).
[5]R. Sayós, J. Hernando, J. Hijazo, and M. González, Phys. Chem. Chem. Phys. **1**, 947 (1999).
[6]R. Sayós, J. Hernando, R. Francia, and M. González, Phys. Chem. Chem. Phys. **2**, 523 (2000).
[7]B. Y. Tang, B. H. Yang, K. L. Han, R. Q. Zhang, and J. Z. Zhang, J. Chem. Phys. **113**, 10105 (2000).
[8]M. P. Deskevich, M. Y. Hayes, K. Takahashi, R. T. Skodje, and D. J. Nesbitt, J. Chem. Phys. **124**, 224303 (2006).
[9]M. Y. Hayes, M. P. Deskevich, D. J. Nesbitt, K. Takahashi, and R. T. Skodje, J. Phys. Chem. A **110**, 436 (2006).
[10]G. Quéméner and N. Balakrishnan, J. Chem. Phys. **128**, 224304 (2008).
[11]S. Yin, M. Guo, L. Li, Y. Zhang, and X. Li, Int. J. Quantum Chem. **111**, 4400 (2011).
[12]P. Defazio and C. Petrongolo, J. Phys. Chem. A **113**, 4208 (2009).
[13]A. Li, H. Guo, Z. Sun, J. Kłos, and M. H. Alexander, Phys. Chem. Chem. Phys. **15**, 15347 (2013).
[14]Z.-X. Duan, M.-H. Qiu, and C.-X. Yao, Comput. Theor. Chem. **1024**, 69 (2013).
[15]E. Wurzberg, A. J. Grimley, and P. L. Houston, Chem. Phys. Lett. **57**, 373 (1978).
[16]E. Wurzberg and P. L. Houston, J. Chem. Phys. **72**, 5915 (1983).
[17]C. M. Moore, I. W. M. Smith, and D. W. A. Stewart, Int. J. Chem. Kinet. **26**, 813 (1994).
[18]A. M. Zolot and D. J. Nesbitt, J. Chem. Phys. **127**, 114319 (2007).
[19]P. Beadle, M. R. Dunn, N. B. H. Jonathan, J. P. Liddy, and J. C. Naylor, J. Chem. Soc., Faraday Trans. 2 **74**, 2170 (1978).
[20]A. M. G. Ding, L. J. Kirsch, D. S. Perry, J. C. Polanyi, and J. L. Schreiber, Faraday Discuss. **55**, 252 (1973).
[21]Z. Sun, S. Y. Lee, and D. Zhang, Chin. J. Chem. Phys. **20**, 365 (2007).
[22]N. Bulut, J. Kłos, and M. H. Alexander, J. Chem. Phys. **136**, 104304 (2012).
[23]S. Gómez-Carrasco and O. Roncero, J. Chem. Phys. **125**, 054102 (2006).
[24]A. Zanchet, O. Roncero, T. González-Lezana, A. Rodríguez-López, A. Aguado, C. Sanz-Sanz, and S. Gómez-Carrasco, J. Phys. Chem. A **113**, 14488 (2009).
[25]A. Zanchet, B. Godard, N. Bulut, O. Roncero, P. Halvick, and J. Cernicharo, Astrophys. J. **766**, 80 (2013).
[26]A. Zanchet, T. González-Lezana, A. Aguado, S. Gómez-Carrasco, and O. Roncero, J. Phys. Chem. A **114**, 9733 (2010).
[27]F. J. Aoiz, V. Sáez-Rábanos, B. Martínez-Haya, and T. González-Lezana, J. Chem. Phys. **123**, 094101 (2005).
[28]M. Alagia, N. Balucani, L. Cartechini, P. Casavecchia, G. G. Volpi, F. J. Aoiz, L. Banares, T. C. Allison, S. L. Mielke, and D. G. Truhlar, Phys. Chem. Chem. Phys. **2**, 599 (2000).
[29]J. M. Bowman, Adv. Chem. Phys. **61**, 115 (1985).
[30]S. Gómez-Carrasco, L. Gónzález-Sánchez, N. Bulut, O. Roncero, L. Banares, and J. F. Castillo, Astrophys. J. **784**, 55 (2014).
[31]D. Skouteris, J. F. Castillo, and D. E. Manolopoulos, Comput. Phys. Commun. **133**, 128 (2000).
[32]C. L. Russell and D. E. Manolopoulos, Chem. Phys. Lett. **256**, 465 (1996).
[33]T. R. Ravuri, V. A. Mandelshtam, and H. S. Taylor, Phys. Rev. Lett. **70**, 1932 (1993).
[34]T. Takayanagi and A. Wada, Chem. Phys. Lett. **348**, 514 (2001).
[35]M. Paniagua, A. Aguado, M. Lara, and O. Roncero, J. Chem. Phys. **111**, 6712 (1999).
[36]T. Gonzalez-Lezana *et al.*, J. Chem. Phys. **123**, 194309 (2005).
[37]U. Fano, Phys. Rev. **124**, 1866 (1961).
[38]C. Kubach, G. Nguyen, and M. Richard-Viard, J. Chem. Phys. **94**, 1929 (1991).
[39]N. Rougeau, S. Marcotte, and C. Kubach, J. Chem. Phys. **105**, 8653 (1996).
[40]S. Gómez-Carrasco, L. González-Sánchez, A. Aguado, O. Roncero, J. M. Alvariño, M. L. Hernández, and M. Paniagua, J. Chem. Phys. **121**, 4605 (2004).
[41]C. Sanz, O. Roncero, A. Aguado, and M. Paniagua, J. Chem. Phys. **119**, 10088 (2003).